

Synthesis, X-ray Structure Determination, and Reactions of (Pentamethylcyclopentadienyl)(nitrosyl)ruthenium η^2 -Arene Complexes

Christopher D. Tagge and Robert G. Bergman*

Contribution from the Department of Chemistry, University of California, Berkeley, California 94720-1460

Received November 3, 1995. Revised Manuscript Received May 3, 1996[⊗]

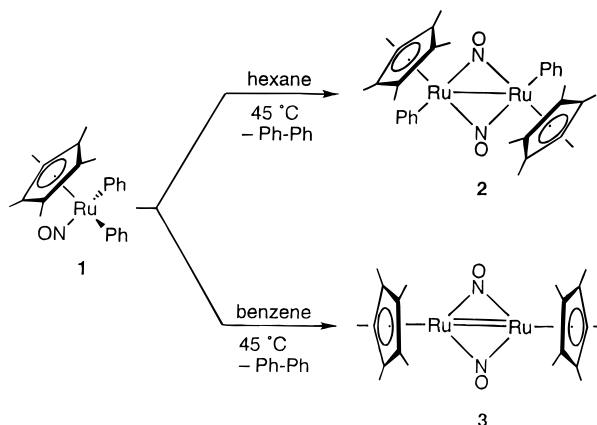
Abstract: The thermally induced reductive elimination of biphenyl from Cp*Ru(NO)Ph₂ (**1**) has been reinvestigated. Careful monitoring of the reaction in aromatic solvents by ¹H NMR spectroscopy has revealed the presence of intermediate Cp*Ru(NO)(η^2 -arene) complexes (**4a**, arene = benzene; **4b**, arene = toluene). Complexes **4** were independently prepared from Cp*Ru(NO)(Me)(OTf) (**5**) and LiHBEt₃ in benzene with loss of CH₄ and LiOTf. At 25 °C added naphthalene displaced the bound arene to generate Cp*Ru(NO)(η^2 -naphthalene) (**6**). The crystal structure of complex **6** has been determined; it crystallizes in triclinic space group *P*1̄, with *a* = 8.6333(16) Å, *b* = 9.8642(10) Å, *c* = 11.2055(13) Å, β = 80.551(13)°, *V* = 870.6(2) Å³, and *Z* = 2. The ligand substitution and oxidative addition reactions of **6** with several organic substrates have been investigated. A kinetic study has shown that the reactions of **6** with phosphines, triphenylsilane, and dimethyl disulfide require initial naphthalene dissociation. The oxidative addition of diaryl disulfides also occurs, but the mechanism is more complicated. We suggest that the reaction of **6** with diaryl disulfide (aryl = Ph, *p*-tolyl) is catalyzed by a small concentration of a secondary product.

Introduction

Coordinationally unsaturated d⁸ metal complexes have been the subject of extensive investigations due to their extraordinary reactivity.^{1–3} Many of these complexes have been generated only as transient intermediates; often, insertion into the C–H bonds of aromatic and aliphatic solvents is extremely fast. It has long been suspected that activation of aromatic C–H bonds involves the formation of an intermediate η^2 -arene complex.^{4,5} Thus, there has been much interest in arresting the reaction of d⁸ metal complexes with arenes at the η^2 -coordination stage.^{6–9}

Chang and Bergman and Hubbard and co-workers have implicated the transient Cp*Ru(NO) 16-electron d⁸ complex as the highly reactive intermediate resulting from the reductive elimination of biphenyl from Cp*Ru(NO)Ph₂ (**1**).^{10,11} While the intermediate could not be detected, its presence was inferred by trapping experiments with phosphines. In the absence of trapping agents, the products of the thermolysis of **1** are highly dependent on the nature of the solvent.¹⁰ In *n*-hexane the major organometallic product is [Cp*Ru(μ -NO)(Ph)]₂ (**2**), resulting from the insertion of the transient Cp*Ru(NO) fragment into the Ru–Ph bond of **1** (Scheme 1). In benzene the transient intermediate appears to be stabilized, dimerizing to form [Cp*Ru(μ -NO)]₂ (**3**) rather than attacking starting material **1**.

Scheme 1



In our effort to understand the oxidative addition reactions of the Cp*Ru(NO) fragment we have obtained direct evidence for the generation of η^2 -arene complexes as intermediates in the thermolysis of complex **1** in aromatic solvents. We have now found methods for generating three η^2 -arene complexes of the Cp*Ru(NO) fragment, rare examples of such species involving d⁸ metal centers, and characterization of one of these (the η^2 -naphthalene complex) by X-ray diffraction. We have used these materials to investigate substitution and oxidative addition reactions of several organic substrates, including disulfides, at the ruthenium center. A kinetic study implicates a simple arene dissociation/oxidative addition mechanism for triphenylsilane and dialkyl disulfides, but a more complicated mechanism for diaryl disulfides.

Results

Synthesis and Characterization of η^2 -Arene Complexes.

In the absence of trapping reagents, careful monitoring of the thermolysis of **1** by ¹H NMR in aromatic solvents (benzene and

[⊗] Abstract published in *Advance ACS Abstracts*, July 1, 1996.

(1) For leading references, see the following two reviews (refs 2 and 3).

(2) Jones, W. D. In *Activation and Functionalization of Alkanes*; Hill, C. L., Ed.; John Wiley and Sons, Inc.: New York, 1989; Vol. I, pp 111–150.

(3) Arndtsen, B. A.; Bergman, R. G.; Mobley, T. A.; Peterson, T. H. *Acc. Chem. Res.* **1995**, *28*, 154–162.

(4) Chatt, J.; Davidson, J. M. *J. Chem. Soc.* **1965**, 843.

(5) Hodges, R. J.; Garnett, J. L. *J. Phys. Chem.* **1968**, *72*, 1969.

(6) Jones, W. D.; Feher, F. J. *J. Am. Chem. Soc.* **1984**, *106*, 1650–1663.

(7) Chin, R. M.; Dong, L.; Duckett, S. B.; Partridge, M. G.; Jones, W. D.; Perutz, R. N. *J. Am. Chem. Soc.* **1993**, *115*, 7685.

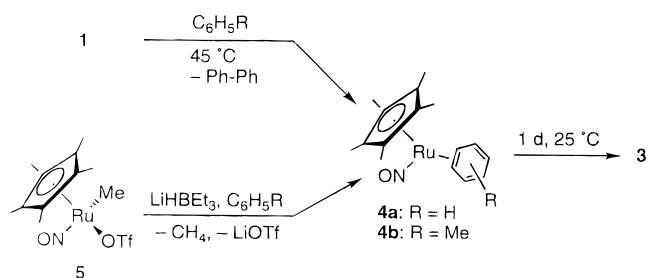
(8) Belt, S. T.; Duckett, S. B.; Helliwell, M.; Perutz, R. N. *J. Chem. Soc., Chem. Commun.* **1989**, 928.

(9) Belt, S. T.; Helliwell, M.; Jones, W. D.; Partridge, M. G.; Perutz, R. N. *J. Am. Chem. Soc.* **1993**, *115*, 1429.

(10) Chang, J.; Bergman, R. G. *J. Am. Chem. Soc.* **1987**, *109*, 4298.

(11) Hubbard, J. L.; Morneau, A.; Burns, R. M.; Zoch, C. R. *J. Am. Chem. Soc.* **1991**, *115*, 9176–9180.

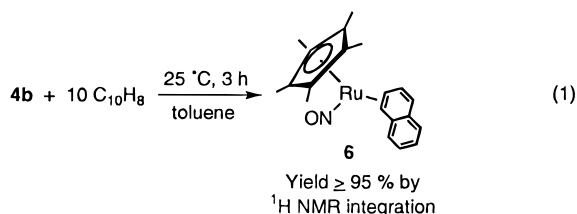
Scheme 2



toluene-*d*₈) revealed the formation and disappearance of a small concentration of a very reactive intermediate. As no transient was detected in aliphatic solvents or THF, we attributed the stability of the intermediate to the aromatic solvent and tentatively assigned the structure as η^2 -benzene complex **4a** (Scheme 2). The fact that no intermediate was observed in THF (an excellent donor but poor π -acceptor ligand) indicates that the ruthenium center is relatively electron-rich and is stabilized by π -acceptance by the η^2 -arene ligand.

Complexes **4** were generated cleanly in much higher concentration by treatment of ruthenium methyl triflate **5** with LiHBET₃ in aromatic solvent (Scheme 2).¹² The ¹H NMR spectrum of **4a** displays two singlets in the ratio of 15 to 6 at δ 1.63 and 6.00, corresponding to the Cp* and the fluxional η^2 -benzene ligand, respectively. The ¹³C NMR spectrum exhibits three resonances at δ 9.94, 95.8, and 105.6. The IR spectrum of **4a** shows an absorbance at 1695 cm⁻¹, indicating the presence of a terminal linear nitrosyl ligand. Complexes **4** are thermally labile and lose arene to form dimer **3** within 24 h in solution at 25 °C.

Our formulation of the structures of **4a** and **4b** is further supported by the complexes' reactions with naphthalene. A toluene solution of **4b**, when treated with 10 equiv of naphthalene at 25 °C for 3 h, led to the formation of Cp*Ru(NO)(1,2- η^2 -naphthalene) (**6**) (eq 1). Thermally, complex **6** is substan-



tially more stable than **4**, and was purified by column chromatography under a nitrogen atmosphere. Crystallization from a hexane/toluene (95/5) solution at -35 °C gave **6** as red blocks in 30% yield. The ¹H NMR spectrum of **6** exhibits a single sharp resonance for the Cp* ligand and eight broad resonances corresponding to a fluxional, unsymmetrically complexed naphthalene ligand. Two of the naphthalene resonances appear well upfield at δ 4.54 and 4.13, indicating η^2 -coordination to the metal center. At -11 °C the fluxional process was sufficiently slowed to allow assignment of the naphthalene resonances based on their coupling constants. The resonances for the α -protons appeared at δ 4.45 (d, 1 H, J_{HH} = 8 Hz) and 4.09 (dd, 1 H, J_{HH} = 8 Hz, J_{HH} = 6 Hz) for the 1 and 2 positions, respectively. The resonances at δ 6.91 (dd, 1 H, J_{HH} = 9 Hz, J_{HH} = 6 Hz) and 6.73 (d, 1 H, J_{HH} = 9 Hz) were assigned to the hydrogens in the 3 and 4 positions of the coordinated naphthalene ring. These resonances are shifted slightly upfield from free naphthalene, indicating a loss of

(12) Treatment of the phenyl analog of **5**, Cp*Ru(NO)(Ph)OTf, with LiHBET₃ in aromatic solvents also led to the formation of an η^2 -arene complex. The presumed intermediate, Cp*Ru(NO)(Ph)H, could not be detected.

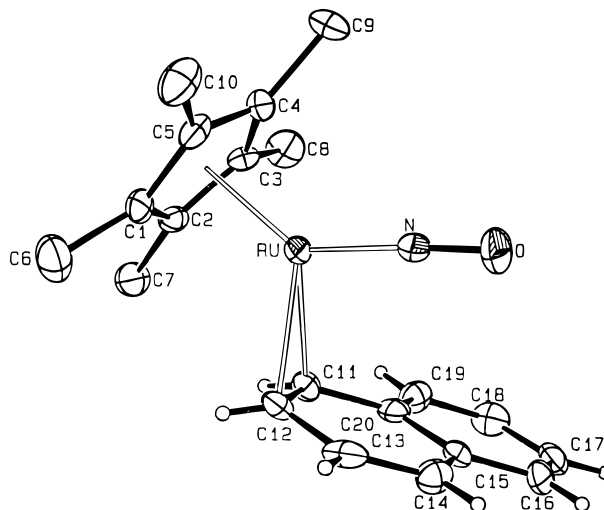


Figure 1. ORTEP drawing of **6**. Ellipsoids are drawn at the 50% probability level. Hydrogen atoms, where represented, are given as arbitrary small spheres for clarity. Selected distances (Å): Ru-C11, 2.195(5); Ru-C12, 2.221(5); C11-C12, 1.418(8); C11-C20, 1.445(7); C12-C13, 1.426(8); C13-C14, 1.346(8); C14-C15, 1.432(7); C15-C20, 1.411(7).

aromatic character for the bound ring. The ¹³C{¹H} NMR spectrum (C₆D₆, 10 °C) exhibits eight distinct resonances for the naphthalene ligand. The IR spectrum of **6** shows a very strong absorption at 1722 cm⁻¹, indicative of a terminal linear nitrosyl ligand.

The solid state structure of **6** was determined by a single crystal X-ray diffraction study (Figure 1). The Ru-C11-C12 plane forms an angle of 115° with the planar naphthalene ligand. The coordinated bond C11-C12 is significantly lengthened (1.418(8) Å) and the α -hydrogens are bent 29° out of the plane of the naphthalene ring. The aromaticity of the bound ring is clearly broken, as the C13-C14 bond length is shorter and the bonds adjacent (C12-C13 and C11-C20) and trans (C14-C15) to the coordinated bond are considerably longer than the corresponding bonds in free naphthalene.¹³ The C-C bond lengths of the unbound ring are similar to those of free naphthalene, showing that the unsymmetrical binding of naphthalene maintains the aromaticity of the free ring.¹³ The terminal nitrosyl ligand is essentially linear, as the Ru-N-O angle is 176°.

As mentioned above, the ¹H NMR resonances of the naphthalene ring in **6** are broad at room temperature, indicating the presence of a dynamic process. From our kinetic studies, we have determined that elevated temperatures (75 °C) are required for significant dissociation of the naphthalene ligand (vide infra). Thus, the broadening of the resonances at room temperature must result from an intramolecular fluxional process. The chemical exchange process was investigated using a phase-sensitive ¹H-¹H two-dimensional exchange (PSEXS) experiment. At low temperature (11 °C) and short mixing time (t_m = 7 ms), the cross-peaks between H1-H4 and H2-H3 in the PSEXS spectrum of **6** indicate exchange between these sites (Figure 2). Thus, the primary fluxional process involves the shift of the ruthenium center from the coordinated bond to the isolated double bond on the same ring. The faint cross-peaks between H1-H2 have dispersive phase and result from scalar coupling between the protons. The absence of cross-peaks between H1-H5 (or H8) indicates that migration of the ruthenium center to the unbound ring of the naphthalene ligand

(13) Foss, L. I.; Syed, A.; Stevens, E. D.; Klein, C. L. *Acta Crystallogr., Sect. C* **1984**, *40*, 272.

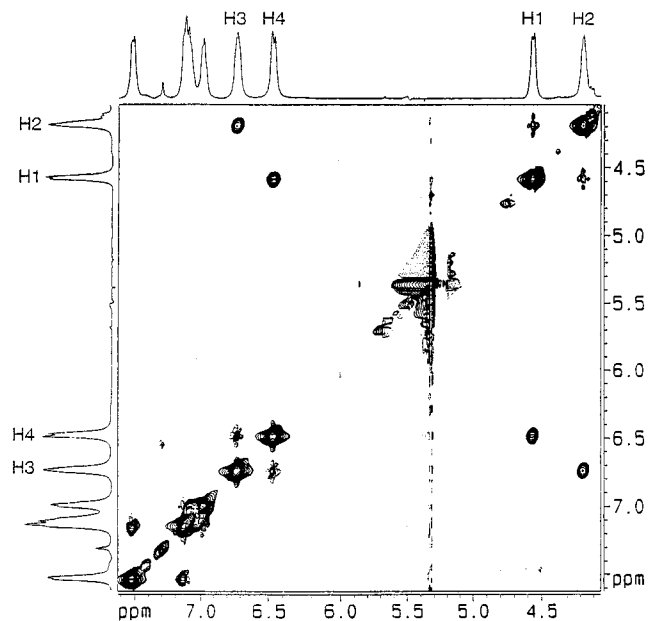
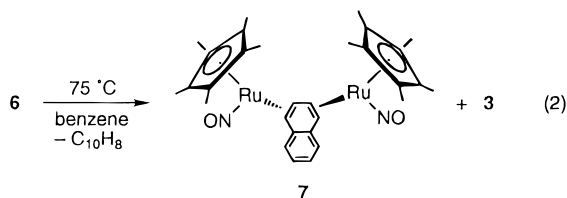


Figure 2. Two-dimensional ^1H - ^1H PSEXS spectrum of **6** acquired at 11 $^\circ\text{C}$ with a mixing time (t_m) of 7 ms.

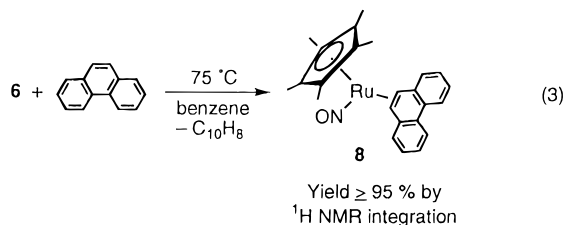
is not significant on the time scale of the PSEXS experiment ($k \leq 10^{-1} \text{ s}^{-1}$).¹⁴

Reactions of 6. Thermolysis of **6** at 75 $^\circ\text{C}$ in aromatic and aliphatic solvents results in the liberation of free naphthalene and formation of a small amount of dimer **3** and a new complex having spectral characteristics consistent with $[\text{Cp}^*\text{Ru}(\text{NO})]_2$ -(1,2- η^2 -3,4- η^2 -naphthalene) (**7**) (eq 2). The ^1H NMR spectrum



of **7** exhibits resonances at δ 1.63 (s, 30 H), 4.00 (d, 2 H, $J_{\text{HH}} = 9$ Hz), 4.53 (d, 2 H, $J_{\text{HH}} = 9$ Hz), 7.05 (dd, 2 H, $J_{\text{HH}} = 6$ Hz, 3 Hz), and 7.46 (dd, 2 H, $J_{\text{HH}} = 6$ Hz, 3 Hz). The integration of the upfield resonances indicates two $\text{Cp}^*\text{Ru}(\text{NO})$ fragments are coordinated to a single naphthalene ligand. The downfield resonances appear as an AA'BB' coupling pattern, characteristic of an ortho-disubstituted aromatic ring, indicating that one ring of the naphthalene ligand retains its aromatic character. Steric interactions should dictate that the two ruthenium fragments are bound on opposite faces of the naphthalene ligand. This type of structure has been observed for the analogous $[\text{CpRh}(\text{PMe}_3)]_2$ -(1,2- η^2 -3,4- η^2 -naphthalene), which has been characterized by X-ray diffraction.¹⁵

Treatment of **6** with phenanthrene at 75 $^\circ\text{C}$ in aromatic and aliphatic solvents leads to the liberation of free naphthalene and the formation of $\text{Cp}^*\text{Ru}(\text{NO})(9,10\text{-}\eta^2\text{-phenanthrene})$ (**8**) in quantitative yield by NMR spectroscopy (eq 3). Complex **8** is



much more thermally stable and was isolated in a much higher yield (when prepared from **4**) than its naphthalene analog. In the ^1H NMR spectrum of **8** the resonances for the protons in the 9 and 10 positions of the phenanthrene ligand appear at δ 4.43 (s, 2 H), indicative of η^2 -coordination. This structure maintains the aromatic character of the two lateral rings of the phenanthrene ligand.

We have found that the above η^2 -arene complexes (**4**, **6**, **7**, and **8**) react in a similar manner with phosphines, triphenylsilane, and dialkyl and diaryl disulfides, differing only in the temperature required for reaction to occur. The preparative reactions were most conveniently conducted with **4**, generated either from thermolysis of **1** or by reduction of **5** in aromatic solvents. The reactions of **6** occurred at temperatures suitable for quantitative kinetic investigations and will be discussed in detail. The reactions of **6** were monitored by ^1H NMR (toluene- d_8 and C_6D_{12}) and UV-visible spectroscopy (heptane).

In the presence of triphenylphosphine, thermolysis of **6** at 75 $^\circ\text{C}$ led to the quantitative formation of free arene and phosphine adduct **9**, which has been previously characterized (Scheme 3).¹⁰ Similarly, thermolysis of **6** with triphenylsilane at 75 $^\circ\text{C}$ in aromatic and aliphatic solvents led to the formation of free naphthalene and ruthenium hydride **10** in excellent yield (Scheme 3). The resonance at δ -5.36 (s, 1 H) in the ^1H NMR spectrum of **10** and the infrared absorbance at 1961 cm^{-1} (w) are characteristic of a ruthenium hydride complex. The terminal linear nitrosyl absorption appears at 1734 cm^{-1} (vs) in the IR spectrum.

Complex **6** reacts with dimethyl disulfide at 75 $^\circ\text{C}$ to give $\text{Cp}^*\text{Ru}(\text{NO})(\text{SMe})_2$ (**11**) in excellent yield (Scheme 4). Similarly, thermolysis of **6** in the presence of $\text{Me}_3\text{CSSCMe}_3$ leads to the corresponding dithiolato complex $\text{Cp}^*\text{Ru}(\text{NO})(\text{SCMe}_3)_2$ (**12**). However, **12** decomposes at the temperature required for its generation from **6**. Complex **12** was obtained in much higher yield from the reaction of $\text{Me}_3\text{CSSCMe}_3$ with **4a** at 45 $^\circ\text{C}$ ($>85\%$ by ^1H NMR integration). Complex **12** was produced on a preparative scale by the treatment of $\text{Cp}^*\text{Ru}(\text{NO})(\text{O}_2\text{C}_2(\text{Me})_4)$ with HSCMe_3 . The ^1H NMR spectrum of **11** exhibits resonances at δ 1.42 (s, 15 H) and 2.54 (s, 6 H) corresponding to the Cp^* and the equivalent methyl groups on the thiolate ligands, respectively. Complex **12** shows resonances at δ 1.40 (s, 15 H) and 1.73 (s, 18 H) in the ^1H NMR spectrum. The IR absorbances due to the terminal linear nitrosyl ligands appear at 1736 (SMe) and 1747 (SCMe_3) cm^{-1} .¹⁶⁻²⁰

The solid state structure of **12** was determined by a single crystal X-ray diffraction study. Complex **12** is a monomeric

(14) Experiments at higher temperature (27 $^\circ\text{C}$) and longer mixing times gave ambiguous results. Cross-peaks between H1-H5 and H1-H8 indicated ruthenium migration to the uncoordinated ring of the naphthalene ligand. However, there is also a significant cross-peak (positive phase) between H1-H2, which could only result from C-H bond cleavage, exchange, and reformation. We have discounted this possibility, as an experiment with 1-deuterionaphthalene showed no scrambling of deuterium atoms to the 2-position of the naphthalene ring. We believe that the chemically unreasonable cross-peaks are artifacts, which may arise from scalar coupling of H1-H2. At this time we can draw no conclusions concerning the validity of the cross-peaks between H1-H5 and H1-H8.

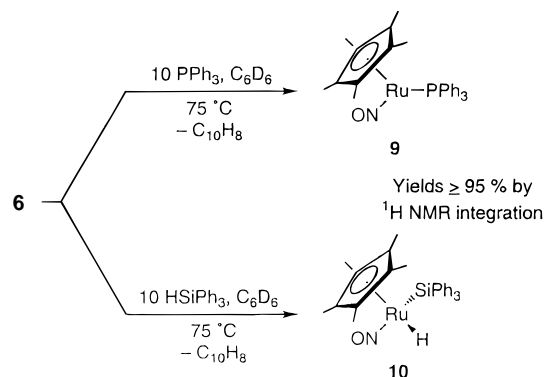
(15) Chin, R. M.; Dong, L.; Duckett, S. B.; Jones, W. D. *Organometallics* **1992**, *11*, 871-876.

(16) We note that the infrared absorptions due to the nitrosyl ligands (1747 cm^{-1} (SCMe_3), 1736 cm^{-1} (SMe), 1723 cm^{-1} (*S-p*-tolyl), and 1728 cm^{-1} (SPh)) for the series of dithiolate complexes progressing from more electron-donating to more electron-withdrawing ligands is not consistent with the trend one would expect for the analogous carbonyl ligand. This is not a solid-state effect, as similar values were obtained in KBr and toluene. Furthermore, the trend does not appear to relate to the steric bulk of the ligands (crystals of **11**, **13**, and **14** suitable for X-ray diffraction could not be obtained, precluding further structural studies). For the monomeric 16-electron complexes $\text{CpMo}(\text{NO})(\text{SR})_2$, no definitive trend was observed for the series ($\text{R} = \text{CHMe}_2$, CH_2Ph , and Ph). We conclude that nitrosyl absorptions are less systematically sensitive than carbonyl absorptions to the electronic environment at the metal center (see refs 17-20).

(17) Ashby, M. T.; Enemark, J. H. *J. Am. Chem. Soc.* **1986**, *108*, 730-733.

(18) James, T. A.; McCleverty, J. A. *J. Chem. Soc. A* **1971**, 1068-1073.

Scheme 3



Scheme 4

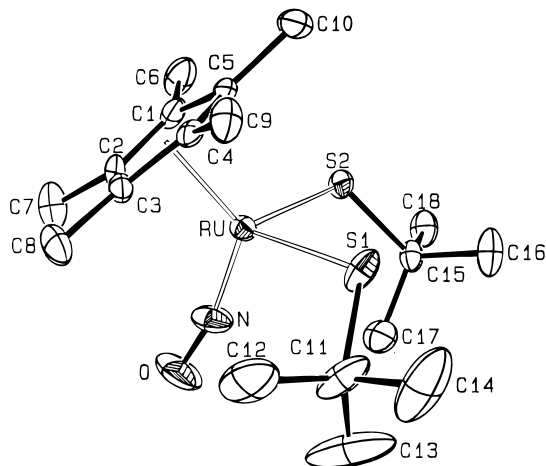
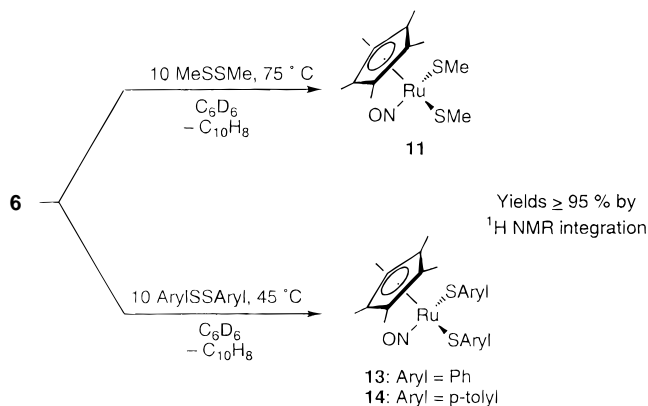


Figure 3. ORTEP drawing of **12**. Ellipsoids are drawn at the 50% probability level.

pseudotetrahedral dithiolate complex (Figure 3). The distance between the two sulfur atoms is 3.25 Å, ruling out S–S interaction. The nitrosyl ligand is essentially linear, with a Ru–N–O angle of 168°. The structure of **12** exhibits a geometry quite distinct from that of the formally 16-electron dithiolate complex CpMo(NO)(SPh)₂.¹⁷ Molecular orbital calculations indicate that the staggered structure of CpMo(NO)(SPh)₂ (the N–Mo–S–Ph torsional angles are 12° and 186°) is stabilized by the overlap between the empty metal d_{xy} orbital and the sulfur 3p lone pair on each thiolate ligand.¹⁷ As **12** is an 18-electron complex, the Ru d_{xy} orbital is filled and overlap with the sulfur 3p lone pair is a repulsive interaction. Thus, the staggered structure is discouraged and the N–Ru–S1–C11 and N–Ru–

S2–C15 torsional angles are 49° and 42°, respectively. Presumably, unfavorable steric interactions between the methyl groups of the Cp* and SCMe₃ ligands prevent further expansion of the N–Ru–S–C torsional angles. Since the N–Ru–S–C torsional angles are not symmetric, one might expect different repulsive interactions between the 3p lone pair of the sulfur ligands with the filled Ru d_{xy} orbital, which could be manifested in bond distances. In fact, this appears to be the case, as the larger torsional angle corresponds to a shorter bond distance. The bond lengths Ru–S1 and Ru–S2 are 2.371 and 2.401 Å, respectively.

In the presence of diaryl disulfides PhSSPh and *p*-tolyl-SS-*p*-tolyl, thermolysis of **6** again leads to the displacement of naphthalene and the formation of dithiolate complexes **13** and **14** (Scheme 4). However, the temperature required for the reaction with diaryl disulfides (25–45 °C) is much lower than that required for the reactions of **6** with dialkyl disulfides. The ¹H NMR spectrum of **13** exhibits resonances at δ 1.21 (s, 15 H), 6.93 (t, 2 H, $J_{\text{HH}} = 7$ Hz), 7.03 (vt, 4 H, $J_{\text{HH}} = 7$ Hz), and 7.68 (d, 4 H, $J_{\text{HH}} = 7$ Hz) consistent with the formulated dithiolate structure. The infrared absorbances for the nitrosyl ligands of **13** and **14** appear at 1728 and 1723 cm⁻¹, respectively. The thiolate ligands of **11**–**14** exchange rapidly at room temperature, precluding any crossover experiments involving RSSR and R'SSR'.

Kinetics. Detailed kinetic studies have been carried out for the reaction of **6** with PPh₃, HSiPh₃, MeSSMe, and diaryl disulfides. Each of these reactions was analyzed by examining the rate of conversion of **6** to product under pseudo-first-order conditions ($[\mathbf{6}] = 1.12 \times 10^{-4}$ M; [naphthalene] = 3.61×10^{-3} M) and then measuring the first-order rate constants k_{obs} at different concentrations of entering organic compound. The most straightforward kinetics were obtained in the PPh₃ substitution and the Ph₃SiH and MeSSMe oxidative addition reactions. The disappearance of **6** was monitored at 75 °C in heptane by UV–visible spectroscopy at 362 nm. Under these conditions the reactions gave complete and clean conversion to phosphine complex **9**, silyl hydride **10**, and dithiolate **11**; excellent first-order behavior in **6** was observed. Rates measured with variable concentrations of naphthalene and entering organic ligand showed that the rates were accelerated by added substrate and inhibited by naphthalene. A plot of k_{obs} vs the ratio of [PPh₃], [HSiPh₃], or [MeSSMe] to [naphthalene] showed clear saturation kinetics at high concentrations of entering organic ligand (Figure 4a). From the intercept of the inverse plot of $1/k_{\text{obs}}$ vs [naphthalene]/[MeSSMe] the rate at saturation was calculated ($k_{\text{sat}} = 4.86 \times 10^{-4}$ s⁻¹) (Figure 4b). Similar values were obtained for PPh₃ and HSiPh₃ ($k_{\text{sat}} = 5.26 \times 10^{-4}$ and 4.72×10^{-4} s⁻¹, respectively). From a temperature-dependence study of the reaction of **6** with HSiPh₃ under saturation conditions ($[\mathbf{6}] = 8.1 \times 10^{-5}$ M; [naphthalene] = 8.3×10^{-4} M; [HSiPh₃] = 8.26×10^{-3} M; 66–96 °C in heptane), the activation parameters of the reaction were determined: $\Delta H^\ddagger = 27.9 \pm 0.4$ kcal/mol and $\Delta S^\ddagger = 6 \pm 2$ eu.²¹ To investigate the effect of a smaller nucleophile, a single kinetic experiment was conducted with PEt₃ ($[\mathbf{6}] = 1.12 \times 10^{-4}$ M; [naphthalene] = 3.61×10^{-3} M; [PEt₃] = 5.75×10^{-3} M; heptane). Once again, the reaction progressed at 75 °C ($k_{\text{obs}} = 3.39 \times 10^{-4}$ s⁻¹).

As mentioned above, the reaction of **6** with diaryl disulfides takes place at a much lower temperature than required for other substrates. The kinetic behavior of the reaction of **6** with diaryl disulfides under pseudo-first-order conditions was analyzed both by monitoring the appearance of **13** by UV–visible spectroscopy

(19) McCleverty, J. A.; Seddon, D. J. *J. Chem. Soc., Dalton Trans.* **1972**, 2588–2593.

(20) Lang, R. F.; Ju, T. D.; Kiss, G.; Hoff, C. D.; Bryan, J. C.; Kubas, G. J. *Inorg. Chem.* **1994**, *33*, 3899–3907.

(21) Jordan, R. B. *Reaction Mechanisms of Inorganic and Organometallic Systems*; Oxford University Press: New York, 1991.

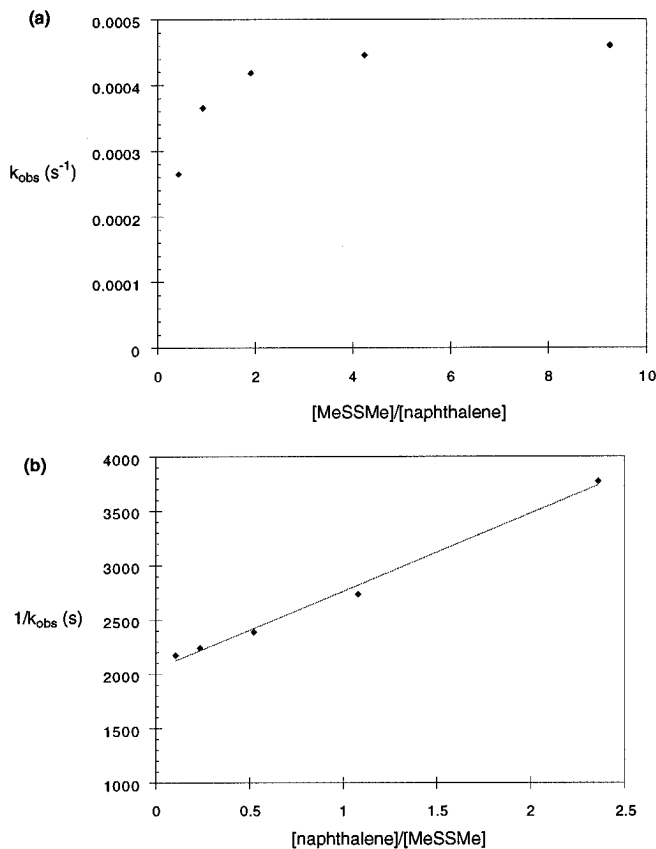


Figure 4. Kinetic data for the reaction of **6** with dimethyl disulfide under pseudo-first-order conditions in heptane at 76 °C: (a) plot of k_{obs} against $[\text{MeSSMe}]/[\text{naphthalene}]$ and (b) the inverse plot.

(*n*-heptane; 45 °C; 484 nm) and monitoring the disappearance of **6** and the appearance of **14** by ¹H NMR spectroscopy (toluene-*d*₈; 45 °C). Care was taken to exclude light from the reaction mixtures, although qualitatively light showed no effect on the reaction rate.

Although at first appearing to proceed analogously to reaction with dialkyl disulfides, reaction of **6** with diaryl disulfides turned out to be surprisingly complicated. The reactions showed apparently clean first-order behavior in both **6** and the dithiolate products; the rate constant for the disappearance of **6** matched well with the rate constant for the growth of **14**. However, repetitive experiments demonstrated that the reaction rates were erratic and so no useful comparison between the effects of aryl substituents could be made. In an attempt to scavenge metal-containing impurities that may have been responsible for this behavior, phosphines were added to the reaction mixture. The reaction of **6** with PhSSPh in the presence of modest concentrations of P(CMe₃)₃ exhibited an induction period (Figure 5) ($[\text{6}] = 1.12 \times 10^{-4}$ M; $[\text{naphthalene}] = 3.61 \times 10^{-3}$ M; $[\text{PhSSPh}] = 8.2 \times 10^{-3}$ M; $[\text{P(CMe}_3)_3] = 8.6 \times 10^{-4}$ M in heptane). In the presence of a large excess of the less sterically encumbered phosphine PET₃ ($[\text{PET}_3] = 2.18 \times 10^{-2}$ in heptane) the reaction of **6** with PhSSPh was effectively stopped at 45 °C, progressing at a moderate rate at 75 °C to give **13**. The phosphine adduct Cp**Ru*(NO)PET₃ may also be formed in the presence of a large excess of PET₃; the UV absorbance of the phosphine complex would be obscured by that of diphenyl disulfide. Added phosphines induced a similar effect on the rate when the reaction was conducted in toluene-*d*₈, although a sufficient concentration of a phosphine to effectively stop the reaction of **6** with diaryl disulfides at temperatures below 75 °C was not reached. No intermediates were detected by ¹H NMR spectroscopy.

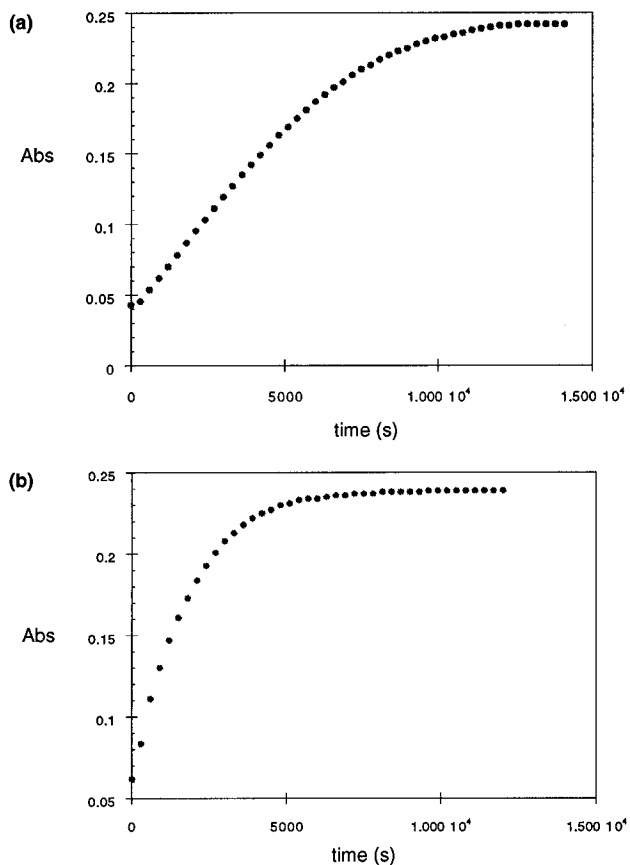


Figure 5. Kinetic data for the reaction of **6** with diphenyl disulfide under pseudo-first-order conditions in heptane at 45 °C: appearance of **13** with respect to time (a) in the presence of P(CMe₃)₃ and (b) in the absence of added phosphines.

Discussion

Structure. Complex **4a** shows a single resonance for the benzene ligand indicating all aromatic protons are equivalent on the NMR time scale. Taube and co-workers have observed similar fluxional behavior for the ruthenium(II) d⁶ complex [(NH₃)₅Ru(η^2 -benzene)](OTf)₂, which exhibited the expected ¹H NMR spectrum for η^2 -binding at low temperature (−87 °C).²² Unfortunately, **4a** is stable only in benzene solution, where the freezing point precludes low-temperature ¹H NMR studies. However, the reaction of **4** with naphthalene and the subsequent isolation and structural characterization of **6** lends credence to our formulation for the structure of **4a**. Spectroscopic and X-ray diffraction data indicate that the complexes **6**, **7**, and **8** adopt the structures predicted as most stable from resonance energy calculations, maintaining as much of the ligand's aromatic character as possible.⁷

Reaction Mechanisms. Transition metal complexes having η^2 -arene ligands are quite rare, especially for d⁸ cyclopentadienyl complexes, where insertion of the metal center into aromatic C–H bonds has limited reactivity studies.² Thus, we undertook a detailed mechanistic investigation of the reactions of **6** with a variety of phosphines and silanes. Because very little is known about the mechanism of oxidative addition of S–S bonds to transition metal centers,^{20,23–25} we extended these studies to the reaction of **6** with dialkyl and diaryl disulfides. As **6** is coordinatively saturated, one would normally expect reactions

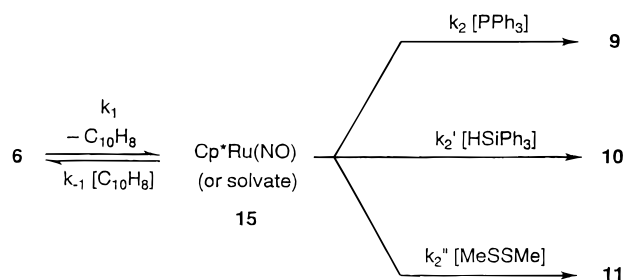
(22) Taube, H. *Pure Appl. Chem.* **1991**, *63*, 651–664.

(23) Aye, K.-T.; Vittal, J. J.; Puddephatt, R. J. *J. Chem. Soc., Dalton Trans.* **1993**, 1835–1839.

(24) Lang, R. F.; Ju, T. D.; Kiss, G.; Hoff, C. D.; Bryan, J. C.; Kubas, G. J. *J. Am. Chem. Soc.* **1994**, *116*, 7917–7918.

(25) Jessop, P. G.; Rettig, S. J.; Lee, C.-L.; James, B. R. *Inorg. Chem.* **1991**, *30*, 4617–4627.

Scheme 5



at the metal center to proceed by a dissociative mechanism. However, both the nitrosyl and pentamethylcyclopentadienyl ligands are capable of changing conformation to open a coordination site, which could allow an associative mechanism.

The saturation kinetic behavior observed for the reaction of **6** with PPh₃, HSiPh₃, and MeSSMe is consistent with the mechanism shown in Scheme 5. The first step is a pre-equilibrium in which naphthalene dissociates from the metal to give a transient species, presumably coordinatively unsaturated Cp*Ru(NO) or its *n*-heptane solvate (**15**).^{2,3,26,27} Subsequent reaction of **15** with the organic substrate generates the corresponding product. Assuming the reverse of the second (k_{-2} , k_{-2}' , k_{-2}'') step in each case remains small enough to be ignored, applying the steady state approximation to the concentration of transient intermediate **15** leads to the rate law shown in eq 4. The inverse form of this equation (eq 5) predicts that plots of

$$\text{Rate} = k_{\text{obs}} [\mathbf{6}] = \frac{k_1 k_2 [\text{Trap}]}{k_{-1} [\text{C}_{10}\text{H}_8] + k_2 [\text{Trap}]} [\mathbf{6}] \quad (4)$$

$$\frac{1}{k_{\text{obs}}} = \frac{k_{-1} [\text{C}_{10}\text{H}_8]}{k_1 k_2 [\text{Trap}]} + \frac{1}{k_2} \quad (5)$$

k_{obs}^{-1} against the ratio of the concentrations of naphthalene to that of entering organic compound should give straight lines (Figure 4b). The rate constant for the dissociation of naphthalene from **6** (k_1) was determined from the intercept of each plot. The agreement of the values derived from the plots for PPh₃, HSiPh₃, and MeSSMe (5.26×10^{-4} , 4.72×10^{-4} , and $4.86 \times 10^{-4} \text{ s}^{-1}$, respectively) indicates that the rate at saturation has no dependence on the identity of the incoming ligand and the rate of naphthalene dissociation from **6** at 75 °C is approximately $5 \times 10^{-4} \text{ s}^{-1}$. The positive activation entropy value ($\Delta S^\ddagger = 6 \pm 2 \text{ eu}$) under saturation conditions is consistent with the dissociative mechanism.

In analogy to their dimethyl analog, diaryl disulfides react with **6** to give the corresponding dithiolato ruthenium nitrosyls **13** and **14** in high yield (Scheme 4). However, kinetic experiments implicate a mechanism that is much more complicated than the dissociative mechanism described above. Reactions with **6** with diaryl disulfides proceed rapidly at 45 °C, a temperature much lower than that required for dissociation of naphthalene from **6**. The reaction rates are erratic and the reaction is inhibited by phosphine. There are only two mechanisms by which phosphine could inhibit the reaction of **6** with diaryl disulfides: (1) reaction with **6** to form an adduct of comparable stability to **6**, so that its concentration increases, and (2) scavenging a catalyst. As no adduct was detected spectroscopically and the rates of the disappearance of **6** and the appearance of the dithiolate product were comparable, we conclude that phosphine must scavenge a highly active catalyst. Attempts to identify the catalytic species have been frustrating.

The reaction is not catalyzed by the dithiolate product, as an induction period was still observed when **14** was added to the reaction of **6** with di(*p*-tolyl) disulfide in the presence of P(CMe₃)₃. We conclude that the reaction generates a low concentration of a secondary product that is a highly active catalyst for the reaction of **6** with diaryl disulfides. Added phosphines scavenge this product, inhibiting the catalytic process. As a large excess of phosphine is needed to completely sequester the catalyst, phosphine coordination must be reversible. In the presence of a large excess of phosphine, where the catalytic reaction is strongly inhibited, the reaction probably proceeds by the (slower) dissociative mechanism observed for dimethyl disulfide.

Summary

We have obtained compelling spectroscopic evidence for the formation of a rare example of a η^2 -benzene complex of a d⁸ metal complex and have structurally characterized its η^2 -naphthalene analog. The ability to prepare η^2 -arene complexes has provided a convenient way to examine oxidative addition reactions in the Cp*Ru(NO) system. The η^2 -naphthalene complex reacts with phosphines, triphenylsilane, and dialkyl disulfides by reversible dissociation of the naphthalene ligand to generate the coordinatively unsaturated intermediate or its solvate, which is quickly trapped by the incoming substrate. The reaction of the η^2 -naphthalene complex with diaryl disulfides produces a very small amount of a secondary product, which catalyzes the conversion to the oxidative addition product.

Experimental Section

General. For a description of the instrumentation and general procedures used, please see earlier papers from these laboratories.²⁸

Unless otherwise specified all reagents were purchased from commercial suppliers and used without subsequent purification. Diethyl ether, toluene, hexamethyldisiloxane, THF, heptane, and benzene were distilled from sodium benzophenone ketyl under nitrogen. Pentane and hexane were distilled from sodium benzophenone ketyl and tetraglyme under nitrogen. Methylene chloride was distilled from calcium hydride under nitrogen. Toluene-*d*₈, benzene-*d*₆, and cyclohexane-*d*₁₂ were vacuum transferred from sodium benzophenone ketyl. Chloroform-*d*₁ was vacuum transferred from calcium hydride. Naphthalene, phenanthrene, and triphenylsilane were purified by sublimation. Dimethyl disulfide was dried over 4 Å molecular sieves. Diphenyl disulfide and di(*p*-tolyl) disulfide were recrystallized from ether at -35 °C under nitrogen. Cp*Ru(NO)Ph₂,¹⁰ Cp*Ru(NO)Cl₂,¹¹ and Cp*Ru(NO)(Me)(OTf)²⁹ were prepared according to the literature procedures.

Spectroscopic Characterization of Cp*Ru(NO)(η^2 -C₆H₆) (4a). A 5-mm NMR tube was charged with **5** (0.010 g, 0.023 mmol), ferrocene as an internal standard (0.005 g, 0.028 mmol), and benzene-*d*₆ (0.5 mL) under nitrogen. The solution was cooled to 10 °C and LiHBEt₃ (1 M in THF, 0.024 mL, 0.024 mmol) was added by syringe. The tube was capped with a rubber septum and parafilm and was immediately transferred to an NMR probe. Integration of the Cp* peak against the internal standard indicated the yield of **4a-d**₆ was 55%. No other products could be discerned. Complex **4a** was prepared in the same manner as its deuterated analog. Spectroscopic data for **4a**: ¹H NMR (400 MHz, C₆H₆, 296 K): δ 1.63 (s, 15H), 6.00 (s, 6H). ¹³C-{¹H} NMR (101 MHz, C₆H₆, 296 K): δ 9.94, 95.8, 105.6. IR (C₆H₆): 1695 (vs), 1068 (m), 914 (w) cm⁻¹.

Cp*Ru(NO)(1,2- η^2 -C₁₀H₈) (6) and [Cp*Ru(NO)]₂(1,2- η^2 -3,4- η^2 -C₁₀H₈) (7). A 30-mL glass bomb was charged with **5** (0.150 g, 0.340 mmol), naphthalene (0.600 g, 4.69 mmol), and toluene (10 mL) under nitrogen. The red solution was cooled to -40 °C, LiHBEt₃ (1 M in THF, 0.31 mL, 0.31 mmol) was added by syringe, and the mixture was stirred for 30 min. The solution turned brownish yellow and a

(26) Mobley, T. A.; Schade, C.; Bergman, R. G. *J. Am. Chem. Soc.* **1995**, *117*, 7822–7823.

(27) Hester, D. M.; Sun, J. M.; Harper, A. W.; Yang, G. K. *J. Am. Chem. Soc.* **1992**, *114*, 5234.

(28) Baranger, A. M.; Bergman, R. G. *J. Am. Chem. Soc.* **1994**, *116*, 3822–3835.

(29) Burns, R. M.; Hubbard, J. L. *J. Am. Chem. Soc.* **1994**, *116*, 9514–9520.

gas was evolved. The mixture was warmed to room temperature over the course of 4 h, stirred for an additional 2 h, and then evaporated to dryness. The residue was dissolved in a hexane/toluene (4/1) solution and chromatographed on a column of silica (10 × 3 cm) under nitrogen. A faint orange band was eluted with hexane/toluene (4/1) and evaporated to dryness (recovered naphthalene, 0.47 g, 84%). A green-yellow band was eluted with hexane/toluene (1/1) and evaporated to dryness (**6**, 0.060 g, 45%). An intense red band was eluted with toluene/hexane (3/1) and evaporated to dryness (**7**, 0.008 g, 8%). Complex **6** was recrystallized from a hexane/toluene solution (3/1, 7 mL) at -35°C to yield orange blocks (0.038 g, 30%). Spectroscopic data for **6**: ^1H NMR (400 MHz, C_6D_6 , 296 K): δ 1.59 (s, 15 H), 4.13 (br, 1 H), 4.54 (br, 1 H), 6.77 (br, 1H), 6.95 (br, 1 H), 7.09 (br, 1 H), 7.21 (br, 1 H), 7.32 (br, 1 H), 7.67 (br, 1 H). ^1H NMR (400 MHz, toluene- d_8 , 268 K): δ 1.61 (s, 15 H), 4.09 (dd, 1 H, $J_{\text{HH}} = 8$ Hz, $J_{\text{HH}} = 6$ Hz), 4.45 (d, 1 H, $J_{\text{HH}} = 8$ Hz), 6.73 (d, 1 H, $J_{\text{HH}} = 9$ Hz), 6.91 (dd, 1 H, $J_{\text{HH}} = 9$ Hz, $J_{\text{HH}} = 6$ Hz), 7.07 (d, 1 H, $J_{\text{HH}} = 8$ Hz), 7.19 (vt, 1 H, $J_{\text{HH}} = 8$ Hz), 7.28 (d, 1 H, $J_{\text{HH}} = 8$ Hz), 7.63 (d, 1 H, 8 Hz). $^{13}\text{C}\{^1\text{H}\}$ NMR (101 MHz, C_6D_6 , 283 K): δ 10.31, 56.41, 58.91, 97.49, 120.97, 124.81, 126.56, 126.65, 127.23, 131.28, 131.94, 141.07. IR (hexanes): $\nu_{\text{NO}} = 1722$ (vs) cm^{-1} . Anal. Calcd for $\text{C}_{20}\text{H}_{23}\text{NORu}$: C, 60.90; H, 5.88; N, 3.55. Found: C, 60.90; H, 6.05; N, 3.58. UV/vis (heptane): $\lambda_{\text{max}} = 362$ nm ($\epsilon = 5270$ L mol^{-1} cm^{-1}). Spectroscopic data for **7**: ^1H NMR (400 MHz, C_6D_6 , 298 K): δ 1.63 (s, 30 H), 4.00 (d, 2 H, $J_{\text{HH}} = 9$ Hz), 4.53 (d, 2 H, $J_{\text{HH}} = 9$ Hz), 7.05 (dd, 2 H, $J_{\text{HH}} = 6$ Hz, 3 Hz), 7.46 (dd, 2 H, $J_{\text{HH}} = 6$ Hz, 3 Hz). ^{13}C NMR (101 MHz, C_6D_6 , 296 K): δ 10.26, 54.56, 60.52, 97.36, 125.12, 126.67, 138.82. IR (C_6D_6): $\nu_{\text{NO}} = 1697$ cm^{-1} (vs). HRMS (EI). m/e calcd for $\text{C}_{30}\text{H}_{38}\text{N}_2\text{O}_2\text{MM}'$: 666.104173 ($M = M' = ^{104}\text{Ru}$), 664.103098 ($M = ^{102}\text{Ru}; M' = ^{104}\text{Ru}$), 663.104332 ($M = ^{101}\text{Ru}; M' = ^{104}\text{Ru}$), 662.102968 ($M = ^{100}\text{Ru}; M' = ^{104}\text{Ru}$), 661.104688 ($M = ^{99}\text{Ru}; M' = ^{104}\text{Ru}$), 660.104490 ($M = M' = ^{101}\text{Ru}$), 659.103613 ($M = ^{99}\text{Ru}; M' = ^{102}\text{Ru}$), 658.104847 ($M = ^{99}\text{Ru}; M' = ^{101}\text{Ru}$), 657.103483 ($M = ^{99}\text{Ru}; M' = ^{100}\text{Ru}$), 656.105203 ($M = M' = ^{99}\text{Ru}$). Found: 666.105499, 664.104877, 663.105818, 662.104248, 661.104439, 660.104221, 659.103946, 658.104436, 657.104471, 657.104253.

CpRu*(NO)(η^2 -phenanthrene) (**8**).** A 30-mL glass bomb was charged with **1** (0.091 g, 0.22 mmol), phenanthrene (0.47 g, 2.6 mmol), and toluene (10 mL) under nitrogen. The mixture was heated at 45°C for 12 h and then evaporated to dryness. The residue was dissolved in a toluene/hexane solution (1/1, 3 mL) and chromatographed on a column of silica (10 cm × 3 cm) under nitrogen. A faint yellow band (phenanthrene) was eluted with toluene/hexane (1/1). A red band was eluted with toluene/hexane (3/1) and evaporated to dryness (0.065 g, 68%). The red solid was recrystallized from toluene/hexanes (3/1, 3 mL) to yield **10** as red crystals (0.047 g, 49%). ^1H NMR (300 MHz, C_6D_6 , 296 K): δ 1.56 (s, 15 H), 4.43 (s, 2 H), 7.14 (vt, 2 H, $J_{\text{HH}} = 8$ Hz), 7.27 (vt, 2 H, $J_{\text{HH}} = 8$ Hz), 7.68 (d, 2 H, $J_{\text{HH}} = 8$ Hz). ^{13}C NMR (101 MHz, C_6D_6 , 296 K): δ 10.19, 56.22, 97.83, 122.88, 124.92, 127.48, 127.62, 129.20, 141.47. IR (toluene): $\nu_{\text{NO}} = 1713$ cm^{-1} (vs). Anal. Calcd for $\text{C}_{24}\text{H}_{25}\text{NORu}$: C, 64.85; H, 5.67; N, 3.17. Found: C, 64.87; H, 5.77; N, 3.26.

CpRu*(NO)(H)SiPh₃ (**10**).** A 30-mL glass bomb was charged with **1** (0.090 g, 0.21 mmol), triphenylsilane (0.450 g, 1.73 mmol), and benzene (8 mL) under nitrogen. The mixture was heated at 45°C for 12 h and then evaporated to a red oil. The oil was diluted with hexane (1 mL) and chromatographed on a column of silica (10 × 2 cm) under nitrogen. A bright yellow band was eluted with benzene/hexane (2/3) and evaporated to dryness (0.079 g, 71%). The yellow solid was recrystallized from a solution of hexane/toluene (95/5, 3 mL) at -35°C to yield **11** as yellow blocks (0.060, 55%). ^1H NMR (400 MHz, C_6D_6 , 296 K): δ -5.36 (s, 1 H), 1.48 (s, 15 H), 7.15 (m, 3 H), 7.25 (m, 6 H), 8.00 (d, 6 H, $J_{\text{HH}} = 8$ Hz). $^{13}\text{C}\{^1\text{H}\}$ NMR (101 MHz, C_6D_6 , 296 K): δ 10.34, 101.08, 127.68, 128.22, 136.84, 141.91. DEPT 45: δ 10.34, 127.68, 128.22, 136.84. IR (KBr): 1734 (vs), 1093 (m), 1427 (m), 1961 (sh), 1979 (m), 2908 (w), 2989 (w), 3062 (w) cm^{-1} . Anal. Calcd for $\text{C}_{28}\text{H}_{31}\text{NORuS}_2$: C, 63.85; H, 5.93; N, 2.66. Found: C, 63.77; H, 6.01; N, 2.79.

CpRu*(NO)(SMe)₂ (**11**).** A 30-mL glass bomb was charged with **1** (0.060 g, 0.14 mmol), dimethyl disulfide (0.45 g, 4.8 mmol), and benzene (8 mL) under nitrogen. The solution was heated at 45°C for 14 h and then evaporated to dryness. The brown residue was dissolved in ether (3 mL) and chromatographed on a column of silica (10 cm ×

2 cm) under nitrogen. A red band was eluted with ether and evaporated to dryness (0.40 g, 80%). The red powder was recrystallized from a toluene/hexane solution (2/7, 8 mL) at -35°C to yield **12** as purple crystals (0.033 g, 66%). ^1H NMR (400 MHz, C_6D_6 , 296 K): δ 1.42 (s, 15 H), 2.54 (s, 6 H). $^{13}\text{C}\{^1\text{H}\}$ NMR (101 MHz, C_6D_6 , 296 K) δ 9.0, 16.0, 107.2. IR (KBr): 1736 (vs), 1400 (m), 2920 (w), 3153 (w) cm^{-1} . Anal. Calcd for $\text{C}_{12}\text{H}_{21}\text{NORuS}_2$: C, 39.98; H, 5.87; N, 3.88. Found: C, 39.81; H, 5.75; N, 3.77.

CpRu*(NO)(O₂C₂(Me)₄).** A 20-mL Schlenk flask was charged with disodium pinacolate (0.031 g, 0.19 mmol), Cp**Ru*(NO)Cl₂ (0.067 g, 0.20 mmol), and cold THF (-35°C , 6 mL) under nitrogen. The mixture was allowed to warm to room temperature, stirred for 30 min, and evaporated to dryness. The brown residue was recrystallized from an ether/hexamethylidisiloxane (1/1, 4 mL) solution at -35°C to yield Cp**Ru*(NO)(O₂C₂(Me)₄) as orange crystals (0.032 g, 42%). ^1H NMR (400 MHz, C_6D_6 , 296 K): δ 1.33 (s, 15 H), 1.34 (s, 6 H), 1.61 (s, 6 H). $^{13}\text{C}\{^1\text{H}\}$ NMR (101 MHz, C_6D_6 , 296 K): δ 8.7, 27.1, 28.6, 87.5, 107.5. IR (C_6D_6): $\nu_{\text{NO}} = 1692$ cm^{-1} (vs). Anal. Calcd for $\text{C}_{16}\text{H}_{27}\text{NO}_3\text{Ru}$: C, 50.24; H, 7.12; N, 3.66. Found: C, 50.47; H, 7.08; N, 3.76.

CpRu*(NO)(SCMe₃)₂ (**12**).** A 20-mL Schlenk flask was charged with Cp**Ru*(NO)(O₂C₂(Me)₄) (0.035 g, 0.092 mmol), HSCMe₃ (0.05 mL, 0.4 mmol), and benzene (5 mL). The mixture was stirred for 1 h and evaporated to dryness. Recrystallization from hexamethylidisiloxane at -35°C gave **12** as brown blocks (0.024 g, 59%). ^1H NMR (300 MHz, C_6D_6 , 296 K): δ 1.39 (s, 15 H), 1.73 (s, 18 H). $^{13}\text{C}\{^1\text{H}\}$ NMR (101 MHz, C_6D_6 , 296 K): δ 9.36, 36.37, 45.91, 107.1. IR (KBr): 1747 (vs), 1026 (w), 1149 (w), 1358 (w), 1379 (w), 1452 (w), 2887 (w), 2850 (w), 2914 (w), 2958 (w) cm^{-1} . IR (toluene): $\nu_{\text{NO}} = 1745$ cm^{-1} (vs). In the mass spectrum (EI) of **12**, peaks having values of m/e corresponding to a dinuclear species were found. Since all other spectroscopic and X-ray diffraction data indicate that **12** is monomeric, we conclude that these dinuclear ions must result from reaction within the source of the mass spectrometer. Furthermore, the isotopic envelope for the molecular ion is complicated by a mixture of M^+ and MH^+ ions. We report only the most intense peak for clarity. HRMS (EI) m/e calcd for $\text{C}_{18}\text{H}_{34}\text{NORuS}_2$: 446.112531 (MH^+ , ^{102}Ru). Found: 446.111676 (MH^+ , ^{102}Ru).

CpRu*(NO)(SC₆H₅)₂ (**13**).** A 30-mL glass bomb was charged with **1** (0.075 g, 0.18 mmol), diphenyl disulfide (0.10 g, 0.46 mmol), and benzene (10 mL) under nitrogen. The mixture was heated at 45°C for 15 h and then evaporated to dryness. The purple solid was washed with pentane (3 × 5 mL), dissolved in CH_2Cl_2 , and filtered through silica. Recrystallization by ether vapor diffusion into a concentrated CH_2Cl_2 solution, followed by storage at -35°C for 2 days, gave **13** as purple needles (0.059 g, 68%). ^1H NMR (400 MHz, CDCl_3 , 296 K): δ 1.58 (s, 15 H), 6.99 (vt, 2 H, $J_{\text{HH}} = 7$ Hz), 7.09 (vt, 4 H, $J_{\text{HH}} = 7$ Hz), 7.41 (d, 4 H, $J_{\text{HH}} = 7$ Hz). ^1H NMR (400 MHz, C_6D_6 , 296 K): δ 1.21 (s, 15 H), 6.93 (vt, 2 H, $J_{\text{HH}} = 7$ Hz), 7.03 (vt, 4 H, $J_{\text{HH}} = 7$ Hz), 7.68 (d, 4 H, $J_{\text{HH}} = 7$ Hz). $^{13}\text{C}\{^1\text{H}\}$ NMR (101 MHz, CDCl_3 , 296 K): δ 9.2, 108.3, 124.2, 127.6, 133.1, 144.1. IR (KBr): 1728 (vs), 690 (m), 739 (m), 1022 (m), 1080 (m), 1375 (m), 1433 (m), 1421 (m), 1576 (m), 2916 (w), 3064 (w) cm^{-1} . UV/vis (heptane): $\lambda_{\text{max}} = 484$ nm. HRMS (EI). m/e calcd for $\text{C}_{22}\text{H}_{25}\text{NORuS}_2$: 487.043180 (M^+ , ^{104}Ru), 485.042106 (M^+ , ^{102}Ru), 484.043339 (M^+ , ^{101}Ru), 483.041976 (M^+ , ^{100}Ru), 482.043695 (M^+ , ^{99}Ru). Found: 487.044227 (M^+ , ^{104}Ru), 485.043907 (M^+ , ^{102}Ru), 484.044051 (M^+ , ^{101}Ru), 483.043768 (M^+ , ^{100}Ru), 482.044304 (M^+ , ^{99}Ru). In the low-resolution mass spectrum (EI) of **13**, peaks were found having values of m/e corresponding to a dinuclear species. Since all other spectroscopic data indicate that **13** is monomeric, we conclude that these dinuclear ions must result from reaction within the source of the mass spectrometer.

CpRu*(NO)(SC₆H₄Me)₂ (**14**).** A 30-mL glass bomb was charged with **1** (0.095 g, 0.23 mmol), di(*p*-tolyl) disulfide (0.16 g, 0.65 mmol), and benzene (10 mL) under nitrogen. The mixture was heated at 45°C for 15 h and then evaporated to dryness. The purple solid was washed with pentane (3 × 5 mL), dissolved in CH_2Cl_2 , and filtered through silica. Recrystallization by ether vapor diffusion into a concentrated CH_2Cl_2 solution, followed by storage at -35°C for 2 days, gave **14** as purple needles (0.053 g, 45%). ^1H NMR (400 MHz, CDCl_3 , 296 K): δ 1.58 (s, 15 H), 2.24 (s, 6 H), 6.90 (d, 4 H, $J_{\text{HH}} = 8$ Hz), 7.30 (d, 4 H, $J_{\text{HH}} = 8$ Hz). $^{13}\text{C}\{^1\text{H}\}$ NMR (101 MHz, CDCl_3 , 296 K): δ 9.2, 21.0, 108.0, 128.5, 133.3, 133.9, 140.2. IR (KBr): 1723

(vs), 801 (m), 809 (m), 1017 (w), 1082 (m), 1483 (m), 2917 (w), 3010 (w) cm^{-1} . IR (toluene): $\nu_{\text{NO}} = 1722 \text{ cm}^{-1}$ (vs). HRMS (EI). m/e calcd for $\text{C}_{24}\text{H}_{29}\text{NORuS}_2$: 515.074480 (M^+ , ^{104}Ru), 513.073406 (M^+ , ^{102}Ru), 512.074639 (M^+ , ^{101}Ru), 511.073276 (M^+ , ^{100}Ru), 510.074996 (M^+ , ^{99}Ru). Found: 515.075638 (M^+ , ^{104}Ru), 513.075333 (M^+ , ^{102}Ru), 512.076114 (M^+ , ^{101}Ru), 511.075922 (M^+ , ^{100}Ru), 510.076258 (M^+ , ^{99}Ru). In the low resolution mass spectrum (EI) of **14**, peaks were found having values of m/e corresponding to a dinuclear species. Since all other spectroscopic data indicate that **14** is monomeric, we conclude that these dinuclear ions must result from reaction within the source of the mass spectrometer.

Thermolysis of 6 with Triphenylsilane: Sample Kinetic Run. In a 10-mL volumetric flask, a mixture of **6** (0.0088 g, 0.022 mmol) and naphthalene (0.0925 g, 0.723 mmol) was diluted to a volume of 10.0-mL with heptane under nitrogen. A 1.0-mL aliquot of this solution was transferred by volumetric pipet to a 10-mL volumetric flask and diluted to a volume of 10.0-mL with heptane. This mixture served as the stock solution of **6**. In a 10-mL volumetric flask, triphenylsilane (0.0141 g, 0.0541 mmol) was diluted to a volume of 10.0 mL with heptane under nitrogen. Aliquots (1 mL) of both the stock solution of **6** and the solution of triphenylsilane were transferred by volumetric pipet to a 4-mL vial. The mixture was shaken vigorously and then transferred by pipet to a 5-mL quartz cell equipped with a stopcock. The cell was placed in a temperature-controlled cell holder, which had been preheated to 76 °C. The reaction was monitored at 300-s intervals to greater than 3.5 half-lives by UV-visible spectroscopy at 362 nm.

X-ray Crystallographic Analysis of CpRu*(NO)(1,2- η^2 -naphthalene) (**6**).** Red blocks of **6** were obtained by slow crystallization from a hexane/toluene (3/1) solution at -35 °C. Fragments cleaved from some of these crystals were mounted on glass fibers using Paratone N hydrocarbon oil. The crystals were then transferred to our Enraf-Nonius CAD-4 diffractometer and centered in the beam. They were cooled to -94 °C by a nitrogen flow low-temperature apparatus which had been previously calibrated by a thermocouple placed at the sample position. Crystal quality was investigated via scans of peaks until a suitable crystal was found. Automatic peak search and indexing procedures yielded a triclinic reduced primitive cell. Inspection of the Niggli values revealed no conventional cell of higher symmetry.

The 2274 unique raw intensity data were converted to structure factor amplitudes and their esd's by correction for scan speed, background, and Lorentz and polarization affects. No correction for crystal decomposition was necessary. Inspection of the azimuthal scan data showed a variation $I_{\text{min}}/I_{\text{max}} = 0.86$ for the average curve. An empirical correction based on the observed variation was applied to the data. The choice of centric group $P\bar{1}$ was confirmed by the successful solution and refinement of the structure.

The structure was solved by Patterson methods and refined via standard least-squares and Fourier techniques. In a difference Fourier map calculated following the refinement of all non-hydrogen atoms with anisotropic thermal parameters, peaks were found corresponding to the positions of most of the hydrogen atoms. Hydrogen atoms (except for the two on the metal-bonded carbons) were assigned idealized locations and values of B_{iso} approximately 1.25 times the B_{eqv} of the atoms to which they were attached. All hydrogens were included in structure factor calculations, but only the hydrogen atoms on the naphthalene were refined. In the final cycles of least squares ten data with abnormally large weighted difference values were given zero weight. These were collected just before one of the reorientations, and it is presumed that they were not completely collected.

The final residuals for 240 variables refined against the 1865 accepted data for which $F^2 > 3\sigma(F^2)$ were $R = 3.12\%$, $wR = 3.48\%$, and $\text{GOF} = 1.34$. The R value for all 2264 accepted data was 4.50%.

The quantity minimized by the least-squares program was $\sum w(|F_o| - |F_c|)^2$, where w is the weight of a given observation. The p -factor, used to reduce the weight of intense reflections, was set to 0.03 throughout the refinement. The analytical forms of the scattering factor tables for the neutral atoms were used and all scattering factors were corrected for both the real and imaginary components of anomalous dispersion.³⁰

Inspection of the residuals ordered in ranges of $\sin(\theta/\lambda)$, $|F_o|$, and parity and value of the individual indexes showed no unusual features or trends. The largest peak in the final difference Fourier map had an electron density of $0.62 \text{ e}^-/\text{\AA}^3$, and the lowest excursion $-0.21 \text{ e}^-/\text{\AA}^3$. There was no indication of secondary extinction in the high-intensity low-angle data.

X-ray Crystallographic Analysis of CpRu*(NO)(SCMe₃)₂ (**12**).** Small, dark tabular crystals of **12** were obtained by slow crystallization from a hexamethyldisiloxane solution at -35 °C. The crystal mounting procedures, diffractometer, and conversion of the raw intensity data to structure factor amplitudes were similar to those described above. Inspection of the intensity standards revealed a reduction of 3.6% of the original intensity. The data were corrected for this decay. Inspection of the azimuthal scan data showed a variation $I_{\text{min}}/I_{\text{max}} = 0.81$ for the average curve. However, there were indications that this variation was overestimated due to misorientation of the crystal during collection of the azimuthal scans. Therefore, an empirical correction was made to the data based on the combined differences of F_{obs} and F_{calc} following refinement of all atoms with isotropic thermal parameters ($T_{\text{max}} = 1.08$, $T_{\text{min}} = 0.94$, no θ dependence).³¹ Inspection of the systematic absences indicated uniquely space group $P2_1/c$. Removal of systematically absent and redundant data left 2771 unique data in the final data set.

The structure was solved by the method described above. In the semi-final difference Fourier map there were indications that two of the methyl groups on the Cp* ligand had disordered hydrogen atoms. These were included at half occupancy (six positions per methyl). The inclusion of the disorder reduced the R -value by 0.15% and the weighted R value by 0.23%.

The final residuals for 208 variables refined against the 2107 data for which $F^2 > 3\sigma(F^2)$ were $R = 2.98\%$, $wR = 3.39\%$, and $\text{GOF} = 1.306$. The R value for all 2771 data was 4.90%.

Acknowledgment. The structural studies were carried out by Dr. F. J. Hollander, director of the U.C. Berkeley X-ray Diffraction facility (CHEXRAY). The PSEXSY experiments were conducted with the help of Dr. Graham Ball. This research was supported by the National Science Foundation through Grant No. CHE-9416833. C.D.T. thanks the National Science Foundation for a predoctoral fellowship.

Supporting Information Available: Tables of crystal, data collection, and positional parameters for **6** and **12**, tables of bond distances and angles, and representative kinetic data (17 pages). See any current masthead page for ordering and Internet access instructions.

JA953711J

(30) Cromer, D. T.; Waber, J. T. *International Tables for X-Ray Crystallography*; The Kynoch Press: Birmingham, England, 1974; Vol. IV.

(31) Walker, N.; Stuart, D. *Acta Crystallogr.* **1983**, A39, 159.